Universitat de Girona
Facultat de Ciències

Ruthenium aqua complexes containing N- and C-donor polypyridilic ligands as catalysts for photocatalytic alcohol oxidation in mild conditions.

Estudiant:*Sergi Danés Pibernat* Grau en *Química*

Correu electrònic: *sdanes96@gmail.com*

Tutor: *Montserrat Rodríguez Pizarro*

Empresa/institució: *Universitat de Girona*

Vistiplau tutor:

Nom del tutor: *Montserrat Rodríguez Pizarro*

Empresa/institució: *Universitat de Girona*

Correu electrònic: montse.rodriguez@udg.edu

Data de dipòsit de la memòria a secretaria de coordinació: *20 de juliol de 2018*

RESUM

Està ben establert que els complexos de ruteni tenen propietats químiques particulars que els fa ser únics. En aquest treball expliquem els diferents tipus de complexos de ruteni i la seva utilitat en diferents àmbits científics. Hem triat dos tipus de cloro- i aquo- complexos de ruteni coneguts per sintetitzar els quals tenen lligands N-donor i C-donors, respectivament, atribuint al complex diferents propietats químiques, electroquímiques i espectrometriques. Els cloro- complexos són els precursors dels aquo-complexos els quals hem avaluat la seva activitat fotooxidativa.

Hem seguit els procediments descrits a la literatura per obtenir els nostres complexos i, alhora, hem dissenyat una nova ruta sintètica per tal de optimitzar i millorar les rutes conegudes. Els productes d'aquestes rutes van ser evaluats per tècniques electroquímiques i espectromètriques comparant les seves diferències entre els dos tipus de complexos i les diferències entre els isomers. L'avaluació fotocatalítica va ser portada a terme amb les mateixes condicions i amb els mateixos substrats amb l'objectiu d'oxidar-los i deduir una relació entre estructura-reactivitat.

RESUMEN

Está bien establecido que los complejos de rutenio tiene propiedades químicas particulares que los hace únicos. En este trabajo exponemos los diferentes tipos de complejos de rutenio y su utilidad en diferentes ámbitos científicos. Hemos triado dos tipos de cloro- i aquo- complejos de rutenio conocidos para sintetizar los cuales tienen ligandos N-dadores i C-dadores, respectivamente, atribuyendo al complejo deferentes propiedades químicas, electroquímicas i espectrométricas. Los cloro- complejos son los precursores de los aquo- complejos los cuales hemos evaluado su actividad fotooxidativa.

Hemos seguido los procedimientos descritos en la literatura para obtener nuestros complejos, y, a la vez, hemos diseñado una nueva ruta sintética para optiizar y mejorar las rutas conocidas. Los productos de estas rutas fueron evaluados per técnicas electroquímicas y espectrométricas, comparando las diferencias entre los dos tipos de complejos i las diferencias entre los isómeros. La evaluación fotocatalítica fue evaluada con las mismas condiciones y con los mismos sustratos con el objetivo de obtener el grupo carbonilo a partir del alcohol de cada sustrato y deducir una relación entre reactividad i estructura.

ABSTRACT

It is well known that ruthenium complexes have particular chemical properties which make them singular. In this work, we report different type of complexes and its usefulness in different scientific areas. We have choosen two type of known chloro- and aquo- polypyridyl ruthenium complexes to synthesize, which have N-donor and C-donor ligands, respectively, leading to the complex distinct chemical, electrochemical and spectrometric properties. The chloro complexes are the precursors aquo complexes which we have evaluated the photooxidative activity.

We have followed a described procedure to obtain our desired complexes and we have designed a new synthetic pathway with the aim to optimize and improve the known synthetic route. The products of these routes were evaluated by electrochemical and spectrometric techniques and we have compared the differences between the two type of complexes and the differences of the isomers of each complexes. The photocathalytic evaluation was employed with two types of aquocomplexes with the same conditions and the same substrates with the aim to obtain a carbonyl group from an alcohol of each substrate, and figure out a relationship between the complex structure and the photocatalytic activity.

Abbreviations

Cb-Me	1-methyl-3-(pyridin-2-yl)-1H-imidazol-3-ium
CV	cyclic voltammetry
d	doublet
dd	double doublet
ddd	double double doublet
DMSO	dimethyl sulphoxide
DPV	differential pulse voltametry
$E_{1/2}$	half wave potential
MLCT	metal to ligand charge transfer
NHC	N-heterocyclic carbenes.
PCET	proton-coupled electron transfer.
pypz-Me	2-(1-methyl-1H-pyrazol-3-yl)pyridine
s	singlet
SET	single electron transfer.
t	triplet
TBAH	tetrabutylammonium hexafuorophosphate
trpy	2,2':6',2"-terpyridine.
UV-Vis	ultraviolet-visible spectroscopy
V	volts
ε	extinction coefficient

Index

1. INTRODUCTION 1
1.1. Ruthenium complexes and their relevance 1
1.1.1 Polypyridyl ruthenium complexes 1
1.1.2 DMSO ruthenium complexes 2
1.1.3 N-heterocyclic carbenes ruthenium complexes 3
1.2. Metalophotocatalysis 3
2. Objectives 6
3. Experimental section 7
3.1. Instrumentation and mesurements 7
3.2. Synthesis of compounds 7
3.3. Linkage isomerization experiments on Ru-DMSO complex 6 12
3.4. Photocatalytic alcohol oxidation experiments 13
4. RESULTS AND DISCUSSION 14
4.1. Synthesis and structure. 14
4.2. UV-vis spectroscopy. 18
4.3. Electrochemical characterization. 18
4.4. Photocatalytic oxidation alcohol reactions 24
5. Conclusions 26
6. Ethics and sustainability 27
7. Bibliography 28

1. INTRODUCTION

1.1. Ruthenium complexes and their relevance

Ruthenium complexes have been widely studied during the last decades due to their particular properties such as the broad accessible range of oxidation states, kinetic stability of different oxidation states and the reversible redox pairs. The different features of the ruthenium complexes depend on the nature of the ligands which are bounded. The ones that have π-conjugate systems are able to dislocate the electronic density of the ruthenium, consequently, they have shown specific properties in nonlinear optics[1], magnetism[2], molecular sensors[3] or liquid crystals[4]. The most employed are the N-donor ligands that give to the complex interesting spectroscopic, photophysical and electrochemical properties. For example, polypyridyl complexes of ruthenium with aqua ligands have been extensively employed in oxidation reaction in organic substrates.

1.1.1 Polypyridyl ruthenium complexes

Professor Meyer has shown that polypyridyl ligands give to ruthenium complexes large stability in different oxidation states from Ru(II) to Ru(V), due to their tolerance to oxidation reactions and the chelation effect to the ruthenium making the complex less susceptible to be decomposed.[5] However, the most important characteristic of this type of complexes is the redox features related on the additional presence of aqua ligands for which a sequential loss of protons goes in parallel with the oxidation of the ruthenium getting, with relative ease, the oxo-ruthenium(IV) complex:

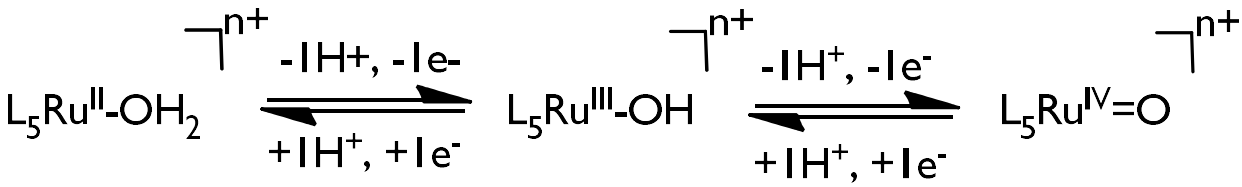

Figure 1. Sequential electron and proton loss from aqua polypyridyl ruthenium complex to oxo polypyridyl ruthenium complex.

This reaction is also known as proton-coupled electron *trans*fer (PCET) and the Ru(IV) is stabilized thanks to the overlap of the p orbitals of the ligand and the d orbitals of the ruthenium.

The potential of these reactions depends on the pH: at low pH, Ru(III)/Ru(II) and Ru(IV)/Ru(III) potentials are higher than in neutral pH conditions whereas, at high pH, the potentials are lower[6], following the Nernst equation:

$$E_{1/2} = E^0_{1/2} - 0.059\,(m/n)\,pH$$

Equation 1. Relation between potential and pH in the Nernst equation. $E_{1/2}$= half wave redox potential at a given pH, $E^0_{1/2}$= half wave redox potential at standard conditions, m= number of *trans*ferred protons, n= number of *trans*ferred electrons.

Furthermore, the process is reversible and the aqua complexes can be usedas oxidation catalysts. The oxo group can attack the substrate and, consequently, it can catalyze different types of oxidations, including wateroxidation.[7 8] The general catalytic process is shown in Figure 2, where a substrate S is oxidized by the Ru^{IV}=O complex that is reduced to Ru^{II}-OH_2.The oxo complex is regenerated by an electron acceptor (oxidant):

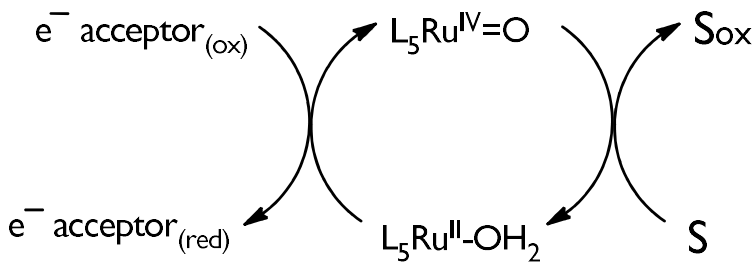

Figure 2. Catalytic cycle for oxidation processes mediated by Ru-OH_2 complexes.

1.1.2 DMSO ruthenium complexes

The DMSO molecule acting as a ligand is usually coordinated by oxygen the group 8, it is coordinated by the sulphur atom. According to the Pearson *hard and soft acids and bases* theory,[9] ruthenium (II) and sulphur are a soft acid and base, respectively, but the oxygen atom is a hard base. So, the d orbitals of the ruthenium (II) overlap better with the π-antibonding orbitals of the S=O bond by sulphur than the oxygen atom. The Ru-S bond is stabilized by the π-backbonding involving the π antibonding orbitals of S=O bond and also empty **d** orbitals of S as π-acceptor, as schematized in Figure 3:

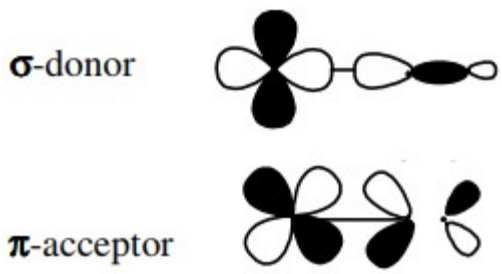

Figure 3. Schematic representation of the orbitals involved in the Ru-S_{DMSO} bonding

The oxidation of Ru(II) to Ru(III) makes the ruthenium ion a harder Lewis acid and in some cases a Ru-S_{DMSO} → Ru-O_{DMSO} linkage isomerization of the

DMSO ligand can been observed, where it coordinates Ru through its O atom.[10] This linkage isomerization is reversed after reduction to Ru(II).

DMSO complexes have an important role in catalysis, for example in hydrogen-atom *trans*fer, hydrogenation,[12] nitrile hydrolysis[13] or oxidation of water[14] and alcohols.[15] In addition these type of complexes are useful for chemotherapeutic agents because of their facility to be hydrolyzed. For example, the NAMI-A complex reduces selectively the formation and growth of lung metastases of malignant tumors.[16]

1.1.3 N-heterocyclic carbenes ruthenium complexes

Carbene complexes have, formally, a double bond between a metal atom and a carbon atom. Carbene complexes are divided in two different groups: Fisher carbenes, which have more affinity for *trans*ition metals of the right side of the d block, and Schrock carbense, which have more affinity to the transition metals situated on the left side of the d block. [17]

NHCs are a privileged type of cationic ligands in transition-metal catalysis due to their excellent σ-donor properties and the π-acceptor character.[18] So, the increase of electron-donating properties obtains new reactivities due to the more π-acidic NHC ligands. Even more NHCs form quite strong metal carbon bond. Therefore, catalysts bearing NHC ligands generally have better air and thermal stability[19].

Moreover, NHCs Ru (II) complexes are able to catalyze oxidation reaction such as olefin epoxidation and water oxidation[20], and oleofin metathesis[21].

1.2. Metalophotocatalysis[22]

Photocatalysis plays a pivotal role in solar energy harvesting, synthesis of clean chemicals, materials development and environmental technology. Traditional photocatalysis primarily focuses on TiO_2 based photocatalysts that absorb limited UV-light but nowadays there is a wide range of new materials that are related with photocatalysis[23]

Metalophotocatalysis is the alliance of transition metal catalysis and photocatalysis which has come out of a novel methodology of synthetic pathways. Photoredox catalysis provides access to reactive radical species under mild condition of wide types of functional groups.

Therefore, metalphotocatalysis provides access to distinct activation modes that are complementary to the traditional transition metal catalysis making possible different catalytic cycles.

The reactivity of *trans*ition metal catalysts can be enhanced and modified using three key design principles:

- Ligand design:

Usually, the ligand design is inspired to the biological systems due to its thermodynamically and kinetically optimization. For example, metalloenzymes routinely perform multielectron reactions near thermodynamic potentials under physiological conditions. The redox-active moieties have finely tuned the potentials and are optimally positioned within metalloenzyme active to promote redox-chemistry[24]. So, the coordinating ligands can essentially modulate the reactivity of the complex, so, it is important to determine the relationship between the structure and activity of a ligand to a given *trans*formation. Even more, for a *trans*ition metal catalysed organic reaction, there is a deeply study in the ligand design with the aim to suit the catalytic cycle.

- *Oxidation state modulation*

The importance of the metal oxidation state in *trans*ition metal catalysts is well established. Indeed, it has long been noted that the acceleration of several elementary steps in coupling protocols can be observed on modulation of the oxidation state of the metal catalyst. As such, a metal centre that is in a higher oxidation state would have a greater thermodynamic driving force to participate in reductive elimination.

- *Catalysts excitation*

The properties of *trans*ition metal species in their excited states have been exploited in many important applications: energy storage, organic light-emitting diodes and dye-sensitized solar cells, to name only a few.

Photoredox catalysis has proves to be highly effective in enabling catalytic access to high-energy oxidation levels and electronically excited states of *trans*ition metal complexes.

Photocatalysis encompasses several mechanistic pathways by which photonic energy is converted into usable chemical energy. A light-absorbing catalyst can, on the excitation, ether remove an electron from or donate an electron to an organic or organometalic substrate. This single-electron *trans*fer (SET) facilitates access to highly reactive radical species under exeptionally mild conditions and can effectively "swich on" other catalysts that are non-functional in the absence of a photocatalyst and visible light.

The use of metal-polypyridyl complexes, absorption corresponds to a metal-to-ligand charge *trans*fer event in which an electron is promoted from a non-bonding metal-centred orbital to the π system of the ligand framework. Subsequent intrensystem crossing leads to the formation of a long-lived triplet excited state. In this configuration, the catalyst possesses both a high-energy electron in a ligand-centred π* orbital and a vacancy in an orbital that is predominantly located on the metal centre. These excited-state catalysts are simultaneously reducing and oxidizing, an unusual

electronic property that provides a powerful tool for the development of new reactivity.

- *Photocatalytic oxidation*

In photosystem II (PSII), water is oxidized by sunlight with the oxygen-evolving complex providing electrons and protons for sustainable processes in nature. The key intermediate of this processs is believed to be highly active manganese(V)-oxo species generated by stepwise PCET[25]. As well, the specie ruthenium (IV)- oxo species have the capacity to oxidate substrates[26] and can be activated by a photosensitizer (Figure 4).

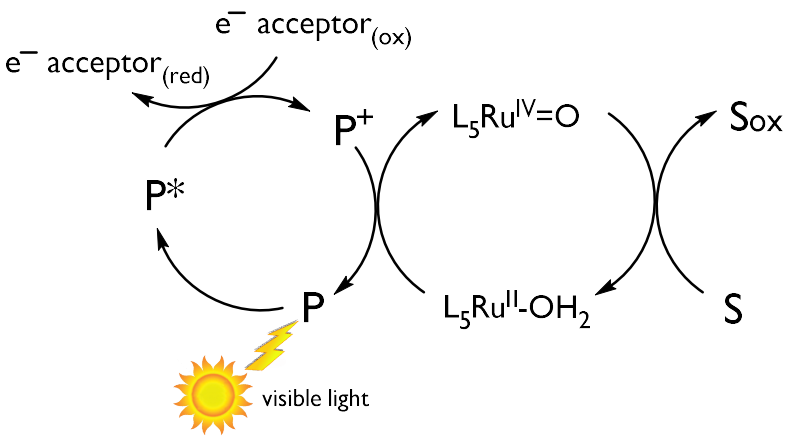

Figure 4 Photocatalytic cycle for oxidation processes mediated by Ru-OH_2 complexes.

2. Objectives

The general objectives of this work were the synthesis of ruthenium complexes with N-donor and C-donor ligands and the evaluation of the complexes as photocatalysts for alcohol oxidation.

The specific objectives are:

- Synthesis and characterization of ruthenium chloro- and aqua-complexes with 2,2′:6′,2″-terpyridine (trpy) and a bidentate ligand D, where D is 2-(3-methyl-1H-3λ^4-imidazol-1yl)pyridine (Cb-Me) or 2-(1-methyl-3H-1λ^4-pyrazol-3-yl)pyridine (pypz-Me, Figure 5):.

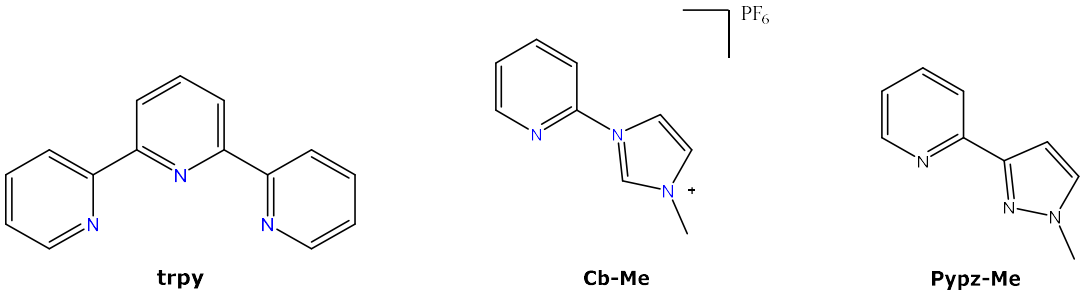

Figure 5. Ligands used in this work

- Optimization of a new synthetic procedure for the preparation of the chloro- and aqua- complexes.
- Evaluation of the photocatalytic activity of the ruthenium aqua complexes synthesized for alcohol oxidation.

3. Experimental section

3.1. Instrumentation and mesurements

- *UV-Vis*

UV-Vis spectroscopy was performed on a Cary 50 Scan (Varian) UV-Vis spectrophotometer with 2mm quartz cells.

- *Cyclic voltammetry (CV) and differential pulse voltametry (DPV)*

CV and DPV experiments were performed in an IJ-Cambria IH-660 potentiostat using a three electrode cell. Glassy carbon electrode (3mm diameter) from BAS was used as working electrode, platinum wire as auxiliary and SCE as the reference electrode. The complexes were dissolved in solvents containing the necessary amount of n-Bu_4NPF (TBAH) as supporting electrolyte to yield a 0.1M ionic strength solution. All $E_{1/2}$ reported in this work were estimated from cyclic voltammetric experiments as the average of the oxidative and reductive peak potentials $(E_{p,a}+E_{p,c})/2$, or directly from DPV peaks.

- *NMR spectra*

The NMR spectroscopy was performed on a Bruker DPX 400 MHz.

- Light emisor

The photocatalytic reactions have been made using the Hananatsu photonics LC8 in which the emitted light was equivalent to the entire spectrum of visible light (400 to 700nm).

3.2. Synthesis of compounds

The synthesis of ligands (HCb-Me)PF_6[27,28] and pypz-Me,[29] as well as the precursor complexes [$RuCl_3$(trpy)] (**1**)[30] and [$RuCl_2$(trpy)(DMSO)] (**6**),[31] have been carried out based on procedures previously described.

Synthesis of ligand 3-methyl-1-(pyridin-2-yl)-1H-imidazol-3-ium hexafluorophosphate, (HCb-Me)PF_6

A sample of 3.16 g (20 mmol) of 2-bromopyridine and 1.64 g (20 mmol) of 1-methylimidazole were added to a round-bottom flask. The mixture was heated at reflux for 48h while vigorous magnetic stirring was maintained. After this time, the reaction was cooled at room temperature. Then, 2 mL of saturated solution of NH_4PF_6 were added to the mixture and a brown precipitate appeared. The solid was filtered in vacuum and washed 3x30mL. Then, the precipitate was purified by flash column chromatography with

alumina eluting with a mixture of hexane/acetone (3:2) increasing the polarity until acetone/hexane (1:4). The yellow fraction obtained corresponds to the methyl-carbene. After column chromatography, the yellow fraction was recrystallized from the mixture with dichlomethane and diethyl ether (1:1), washed with diethyl ether, and dried under vacuum; yield 62.0% (3.828g).

Synthesis of ligand 2-(1-methyl-1H-pyrazol-3-yl)pyridine, pypz-Me.

The synthesis of the pypz-Me ligand has been performed following a procedure previously described. A sample of 2.015g (11 mmol) of 3-dimethylamino-1-(2-pyridyl)-2-propen-1-one and 0.735g (14.3 mmol) of hydrazine were added to round-bottom flask. The mixture was headed at reflux for 1 hour. Afterward, it was cooled at room temperature and, then, the volume was reduced until a brown-red solid appeared corresponding to the 2-(1-methyl-1H-pyrazol-3-yl)pyridine intermediate (pypz-H).

Then, a sample of 0.540g (13.2 mmol) of NaH (60% w/w) was washed with hexane and it was added to a round-bottom flask containing an equimolar amount of pypz-H. Afterward, 30 mL of THF anhydrous were added and the mixture was stirred for 30 minutes at 0ºC. Finally, a sample of 1.944g (13.2mmol) of CH_3I was added and the mixture was headed at 343K while vigorous magnetic stirring was maintained for 48h. A viscous solid appeared and it was dissolved with THF while vigorous magnetic stirring was maintained. 5x20mL of pentane were added to the mixture and poured in another round-bottom flask and the volume was reduced until an orange oil appeared corresponding to the pypz-Me ligand. Then, this oil was recrystallized it THF/ether (1:1) obtaining an orange-brown solid. ^{1}H NMR (300Hz, acetone-d_6) δ(ppm): 8.60 (dq,H1), 7.97 (t, H4), 7.87 (td, H3), 7.73 (d, H10), 6.92 (d, H9), 3.98 (s,H12). The resonances have been assigned following the numbering scheme shown in Figure 8.

Complexes *cis* and *trans*-[RuCl(Cb-Me)(trpy)]PF_6, *cis* and *trans*-2

Two different pathways, A and B, have been followed for the synthesis of isomeric chlorocomplexes **2**. Pathway A is based on a synthetic procedure previously described.[32]

Pathway A

A.1. Synthesis of [Ru(trpy)Cl_3], 1

A sample of 0.216 g of $RuCl_3$·2.53 H_2O and 0.199g of 2,2':6′,2′′-terpyridine were added to 125 mL of methanol in a round-bottom flask. The mixture was heated at reflux for 3 h while vigorous magnetic stirring was maintained. After this time the reaction was cooled at room temperature and the volume of the mixture was reduced at low pressure until appears a

brown precipitate. Then, the precipitate was filtered in vacuum and washed with 3X30mL of diethyl ether. Afterwards, the brown solid was air-dried; yield 80.1% (0.302g).

A.2. Synthesis of [RuCl(Cb-Me)(trpy)]PF_6, 2(PF_6).

A sample of 0.104g (0.2 mmol) [Ru(trpy)Cl_3], **1**, and 0.0506 (1.1 mmol) of LiCl were dissolved in 40mL of a mixture EtOH/H_2O (3:1) under N_2 atmosphere in a 100mL round-bottom flask. Then, 0.06 mL (0.436 mmol) of NEt_3 was added, and the mixture was stirred for 30 min at room temperature, upon which it progressively became a dark solution. At this point, a sample of 0.0553g (0.2 mmol) of (HCb-Me)PF_6 ligand was dissolved in 2mL of degassed solution of EtOH/H_2O (3:1) and added to the dark-green solution, and the resulting solution was refluxed overnight. Upon cooling to room temperature, the solution was filtered on a frit to eliminate small amounts of black solid. Afterward, 3 mL of saturated KPF_6 aqueous solution was added to the mixture, and the volume was reduced at low pressure until a brown precipitate appeared. The resulting solid was filtered on a frit, washed with 3x30mL of ether, and dried in vacuum. The brown solid obtained was purified by chromatography over basic alumina using dichloromethane as eluent and an increasing gradient of methanol (0-1%). A first brown fraction corresponding to the *cis* isomer, a second orange fraction corresponding to $[Ru(trpy)_2]^{2+}$ byproduct, and a third violet fraction corresponding to the *trans* isomer. After column chromatography, *cis* and *trans* isomers were recrystallized with ether. Finally, 9mg of *cis* isomer (yield: 6.7%) and 20 mg of *trans* isomer (yield: 14.9 %) were obtained. For ***trans*-2**: ^{1}H NMR (400MHz, acetone-d_6): δ(ppm)=10.15(ddd, H16), 8.68 (d, H7, H9), 8.57 (dt, H4, H12), 8.31 (m, H19), 8.29 (m, H20), 8.25(d, H23), 8.10 (td, H8), 8.01 (td, H3, H18), 7.77(t, H17), 7.71(dd, H1, H15), 7.36 (t, H2, H14) 7.08 (d, H22), 4.62 (s, H32). $E_{1/2}$(III/II) (CH_2Cl_2+0.1M TBAH) 0.92V vs. SCE. ; UV-Vis (CH_2Cl_2): λ_{max}, nm (ε, M^{-1} cm^{-1}) 268 (19971), 315 (12500), 372 (3571), 480 (2885).

For ***cis*-2**: ^{1}H NMR (400MHz, acetone-d_6): δ(ppm)=8.75 (d, H7, H10), 8.57 (d, H4, H13), 8.50(d, H24), 8.29(t, H9), 8.11(d, H4, H17), 8.00 (d, H20), 7.93 (t, H3, H14), 7.83 (s,H23), 7.75 (t, H23), 7.44(d, H17), 7.31 (t, H2, H15), 6.89 (t, H18), 4.62 (s, H25). $E_{1/2}$(III/II) (CH_2Cl_2+0.1M TBAH) 0.82V vs. SCE ; UV-Vis (CH_2Cl_2): λ_{max}, nm (ε, M^{-1} cm^{-1}) 233 (16890), 240 (sh 13013), 267 (10448), 319 (11367), 386 (3205), 499 (2403).

Pathway B

B.1. Synthesis of *cis* and *trans*-[$RuCl_2$(trpy)(dmso)], 6

A sample of 0.253g (0.5mmol) of [Ru(dmso)$_4Cl_2$] and 0.1226 g (0.5mmol) of 2,2':6′,2′′-terpyridine were added to 40 mL of degassed EtOH solution in a round-bottomed flask of 100mL. The mixture was heated to reflux for 4

hours upon which it progressively became dark brown. The volume was reduced at low pressure until a brown precipitate appeared. Then, the resulting solid was filtered on a frit, washed with 3x30 mL of ether and dried to vacuum. The solid obtained corresponds to a mixture of **6** in a *cis*:*trans* 1:0.35 isomeric ratio. Yield 68% (0.177g).

^{1}H NMR (400MHz, methanol-d) δ(ppm):8.97(d, H1, H15), 8.71 (d, H7, H9), 8.50(t, H8), 8.01 (td, H3, H13), 7.47 (t, H1, H15), 7.27 (ddd, H14, H2), 4.59 (s, H11)

B.2. Synthesis of [RuCl(Cb-Me)(trpy)]Cl, 2(Cl).

A sample of 0.025g (0.052 mmol) of [Ru(dmso)(trpy)Cl_2], **6**, were added to 30mL of degassed EtOH (96% w/w) in a round-bottomed flask of 100mL. Then, 90μL of NEt_3 and 0.0158g (0.052 mmol) of (HCb-Me)PF_6 in 10 mL of degassed EtOH (96% w/w) were added to the mixture and heated to reflux for overnight. After that, the solvent was totally removed at low pressure. The solid was redissolved in 4mL of dicloromethane and then 15mL of ether were added and a brown precipitate appeared. The resulting solid was filtered on a frit, washed with 3x30ml of ether and 3x30mL of pentane and dried in vaccum. The brown solid corresponds to isomerically pure *trans*-[RuCl(Cb-Me)(trpy)]Cl; yield 78% (0.023g).

^{1}H NMR (400MHz, acetone-d_6): δ(ppm)=10.16(d, H16), 8.67 (d, H7, H9), 8.60(d, H4, H12), 8.30 (m, H19, H20), 8.25(d, H23), 8.18(td, H8), 7.99(td, H3, H18), 7.78(m, H17), 7.69 (ddd, H1, H15), 7.36 (m, H2, H14), 7.07 (d, H22), 2.95(s, H24). $E_{1/2}$(III/II) (CH_2Cl_2+0.1M TBAH)=0.90V.

Complexes - *cis* and *trans*-[RuCl(pypz-Me)(trpy)]PF_6, *cis* and *trans*-3.

Two different pathways, A and B, have been followed for the synthesis of isomeric chlorocomplexes **3**. Pathway A is based on a synthetic procedure previously described.[33]

Pathway A

A.1. Synthesis of complex [Ru(trpy)Cl_3], 1

The synthesis of **1** was carried out as described previously for the synthesis of isomeric chlorocomplexes **2** (pathway A).

A.2. Synthesis of [RuCl(pypz-Me)(trpy)]PF_6, 3(PF_6).

A sample of 0.150g (0.22mmol) [Ru(trpy)Cl_3] was added to a 100mL round-bottom flask containing a solution of 0.018 g (0.44mmol) of LiCl dissolved in 40 mL of EtOH/H_2O (3:1) under magnetic stirring. Then, 0.06 mL (0.436 mmol) of NEt_3 was added, and the reaction mixture was stirred at room temperature for 30 min under N_2 and in the darkness upon which it progressively became dark green. At this point, 0.052g (0.218 mmol) were

dissolved in 4mL of degassed solution of EtOH/H_2O (3:1) and added to the dark solution. The mixture was heated to reflux for 3h. The hot solution was filtered off in a frit to eliminate small amounts of a black solid and 3 mL of saturated KPF_6 aqueous solution were added. The volume was reduced at low pressure until a brown precipitate appeared. The resulting solid was filtered off on a frit, washed with 3X30 mL of ether and dried in vacuum. The brown solid was purified by chromatography over silica using a solution of CH_2Cl_2:acetone (9:1). A first brown fraction corresponding to *cis*/*trans*-[RuCl(pypz-Me)(trpy)]PF_6 and a third orange fraction corresponding to [Ru(trpy)$_2$](PF_6)$_2$ were obtained. Finally, 79mg (yield: 59%) of *cis*/*trans*-[RuCl(pypz-Me)(trpy)]PF_6 were obtained. ^{1}H NMR (300Hz, acetone-d$_6$) δ(ppm): 10.17(dq, H26$_{trans}$), 8.73 (d, H10$_{trans}$, H11$_{trans}$), 8.68(d,H22$_{cis}$, H24$_{cis}$), 8.60(tt, H19$_{trans}$, H7$_{trans}$, H18$_{cis}$, H30$_{cis}$), 8.48(dq, H23$_{trans}$), 8.41(d,H8$_{cis}$), 8.29(td, H24$_{trans}$) 8.16(m, H12$_{trans}$, H23$_{cis}$), 8.07(ddd, H1$_{cis}$, H15$_{cis}$), 7.99 (m, H18$_{trans}$, H2$_{trans}$, H13$_{cis}$, H29$_{cis}$), 7.85(td, H25$_{trans}$), 7.44(m, H3$_{trans}$, H17$_{trans}$, H14$_{cis}$, H28$_{cis}$), 7.36(ddd, H1$_{cis}$), 7.20(d,H28$_{trans}$), 7.94(td,H2$_{cis}$), 4.72(s, H32$_{cis}$) 3.02(s, H32$_{trans}$,). $E_{1/2}$(IV/III)$_{Cis/Trans}$ (CH_2Cl_2+0.1M TBAH) 0.87V. UV -Vis (CH_2Cl_2): λ_{max}, nm (ε, M^{-1} cm^{-1}) 262 (13418), 282 (9512.5), 377(3300), 488 (2875).

Pathway B

B.1. Synthesis of *cis* and *trans*-[RuCl$_2$(trpy)(dmso)], 6

The synthesis of **6** was carried out as described previously for the synthesis of isomeric chlorocomplexes **2** (pathway B).

B.2. Synthesis of [RuCl(pypz-Me)(trpy)]Cl, 3(Cl).

A sample of 0.011g (0.02 mmol) of [RuCl$_2$(trpy)(dmso)] and 0.005g (0.02mmol) of pypz-Me were added to 30 mL of degassed EtOH (96% w/w) in a round-bottomed flask of 100mL. The mixture was headed to reflux under N_2 atmosphere and in the darkness overnight. Afterward, the volume was totally reduced at low pressure. The resulting solid was redissolved in 4 mL of dicloromethane, precipitated with 15mL of ether and filtered on a frit, washed with 3x30mL of ether and 3X30mL of pentane and dried to vacuum. The resulting solid corresponds *to trans*-[RuCl(pypz-Me)(trpy)]Cl and some impurities. It was purified by chromatography over basic alumina using dichloromethane as eluent and an increasing gradient of acetone (0-10%) and methanol (0.1-1%). Yield 66% (7.5mg).

NMR (400MHz, acetone-d$_6$): δ(ppm)=10.09(d), 8.60(d), 8.48 (d), 8.23(d), 8.11(t), 7.92(t), 7.82(t), 7.67(t), 7.63(d), 7.31(d), 7.21(t), 6.98(d), 2.84(s). $E_{1/2}$(III/II) (CH_2Cl_2+0.1M TBAH)=0.82V.

Complex *trans*-[Ru(Cb-Me)(trpy)(OH_2)](PF_6)$_2$, *trans*-4

Complex *trans*-**4** has been prepared following a similar procedure to that described for *cis*-**4** but using complex *trans*-[RuCl(Cb-Me)(trpy)]PF_6, *trans*-**2(PF_6)**, as starting material. Yield:55% $E_{1/2}$(IV/II) (phosphate buffer pH=7) 0.64V vs. SCE; UV-Vis (phosphate buffer) λ_{max} (nm): 267, 277(sh), 312, 362, 463.

Complexes *cis* and *trans*-[Ru(pypz-Me)(trpy)(OH_2)](PF_6)$_2$, *cis* and *trans*-5.

A sample of 0.079g (0.11 mmol) of a *cis*/*trans* isomeric mixture of complex [RuCl(pypz-Me)(trpy)]PF_6, **3**, was added to a 50ml round-bottom flask. Then, 6 mL of MilliQ water were added and the reaction mixture was stirred and heated to reflux for 3h. The solution progressively became orange-brown. Afterward, the volume was reduced at low pressure and then 2 ml of KPF_6 were added to the mixture. A dark precipitate appeared and it was cooled in an ice bath. The resulting solid was filtered off on a frit, washed with 3X10mL of ether and 10 mL of pentane, and dried in vacuum. Yield: 62%. ^{1}H NMR (400Hz, D_2O) δ(ppm):9.46 (d, H26$_{trans}$), 8.55 (t, H24$_{trans}$, H22$_{trans}$, H24$_{cis}$, H22$_{cis}$), 8.44 (t, H7$_{trans}$, H19$_{trans}$, H18$_{cis}$, H30$_{cis}$), 8.34(d, H23$_{trans}$), 8.25 (m, H9$_{cis}$, H24$_{trans}$), 8.14 (t, H12$_{trans}$), 8.07 (t, H23$_{cis}$), 8.01 (d, H15$_{cis}$, H27$_{cis}$), 7.95 (m, H2$_{trans}$, H18$_{trans}$, H4$_{cis}$, H14$_{cis}$, H29$_{cis}$), 7.84 (t, H25$_{trans}$), 7.77 (d, H36$_{trans}$, H9$_{trans}$), 7.58 (td, H2$_{cis}$), 7.84(t, H25 $_{trans}$), 7.77 (d, H36 $_{trans}$, H9$_{trans}$), 7.58 (td, H2$_{cis}$), 7.39 (m, H29$_{trans}$, H9$_{cis}$), 7.31 (m, H28$_{cis}$, H19$_{cis}$, H3$_{trans}$, H36$_{trans}$), 7.17 (d, H1$_{cis}$), 6.99 (d, H28$_{trans}$), 6.78 (td, H2$_{cis}$), 4.45 (s, H32$_{cis}$), 2.89 (s, H32$_{trans}$). $E_{1/2}$ (phosphate buffer pH = 7.02, vs SCE): 0.38V Ru(III/II)$_{trans}$, 0.50V Ru(III/II)$_{cis}$ + Ru(IV/III)$_{cis}$, 0.60V Ru(IV/III)$_{trans}$

3.3. Linkage isomerization experiments on Ru-DMSO complex 6

A sample of complex **6** was dissolved in CH_2Cl_2 containing 0.1 M TBAH. Anodic scan CVs were performed starting at 0 V (vs. SCE) with 2 s equilibrium time and scanning the potential up to 1.1 V. Cathodic scan CVs were carried out starting at 1.1 V with 1 minute of equilibrium time and scanning up to 0 V. In both cases the scan rates used were 0.02, 0.05, 0.1, 0.15, 0.2, 0.3, 0.4, 0.5, 0.6, 0.7 and 0.8 V/s. Cathodic and anodic intensity data were treated through the equations displayed in Table 1, following the procedure described in the literature.[34]

Table 1. Equations used for the calculation of rate (k) and equilibrium (K) constants.[a]

$\frac{i_{c1}}{i_{c2}} = \frac{RT}{nF} \cdot \frac{1}{v} + K_{O-S}^{III}$ **(eq. 1)**	$\sqrt{v} = \frac{K_{O-S}^{III}}{0.471 \cdot \sqrt{\frac{nFl}{RT}}} \cdot \frac{i_{a1}}{i_{c1}} + b1$ **(eq. 2)**
$K^{II} = K^{III} + e^{\frac{F}{RT} \cdot (E_{Ru-}^{0} - E_{Ru-}^{0})}$ **(eq. 3)**	$ln\left(\frac{i_{a1}}{\sqrt{v}}\right) = k_{O-S}^{II} \cdot \frac{1}{v} + b2$ **(eq. 4)**

[a] i_{a1} and i_{c1} = anodic and cathodic peak intensities of the original Ru-S_{dmso} complex, respectively (A); i_{c2} = cathodic peak intensity of the Ru-O_{dmso} complex; E^0 = standard potential; T= temperature (298 K); R = Boltzmann constant (8.31 $J \cdot K^{-1} \cdot mol^{-1}$); F = Faraday constant (96500 $A \cdot s \cdot mol^{-1}$); n = number of exchanged electrons; $l = k_{O-S}^{III} + k_{S-O}^{III}$; ν = scan rate (V/s); *b1* and *b2* = intercept values.

3.4. Photocatalytic alcohol oxidation experiments

The photocatalytic experiments were done in a ratio of 1:10:100:200 (catalyst: photosensitizer:substrate:oxidant) in 1.5 mL of phosphate buffer pH=7. The catalysts were *trans*-4 and *cis*-5/*trans*-5, the photosensitizer is $[Ru(bpy)_3]Cl_2$ and the sacrificial oxidant was $Na_2S_2O_8$. The reactions were employed under visible light during 15 hours. Then, the reaction crude was extracted three times with 10 mL of $CHCl_3$. Then the volume of the organic phase was totally reduced at low pressure.

4. RESULTS AND DISCUSSION

4.1. Synthesis and structure.

The synthetic procedure for the preparation of all the complexes is shown in Figure 6. In chloro and aqua complexes **2-5**, the notation *cis* or *trans* indicates the relative position of the five-membered ring of the bidentate ligand (Cb-Me or pypz-Me) and the monodentate (Cl or H_2O) ligand.

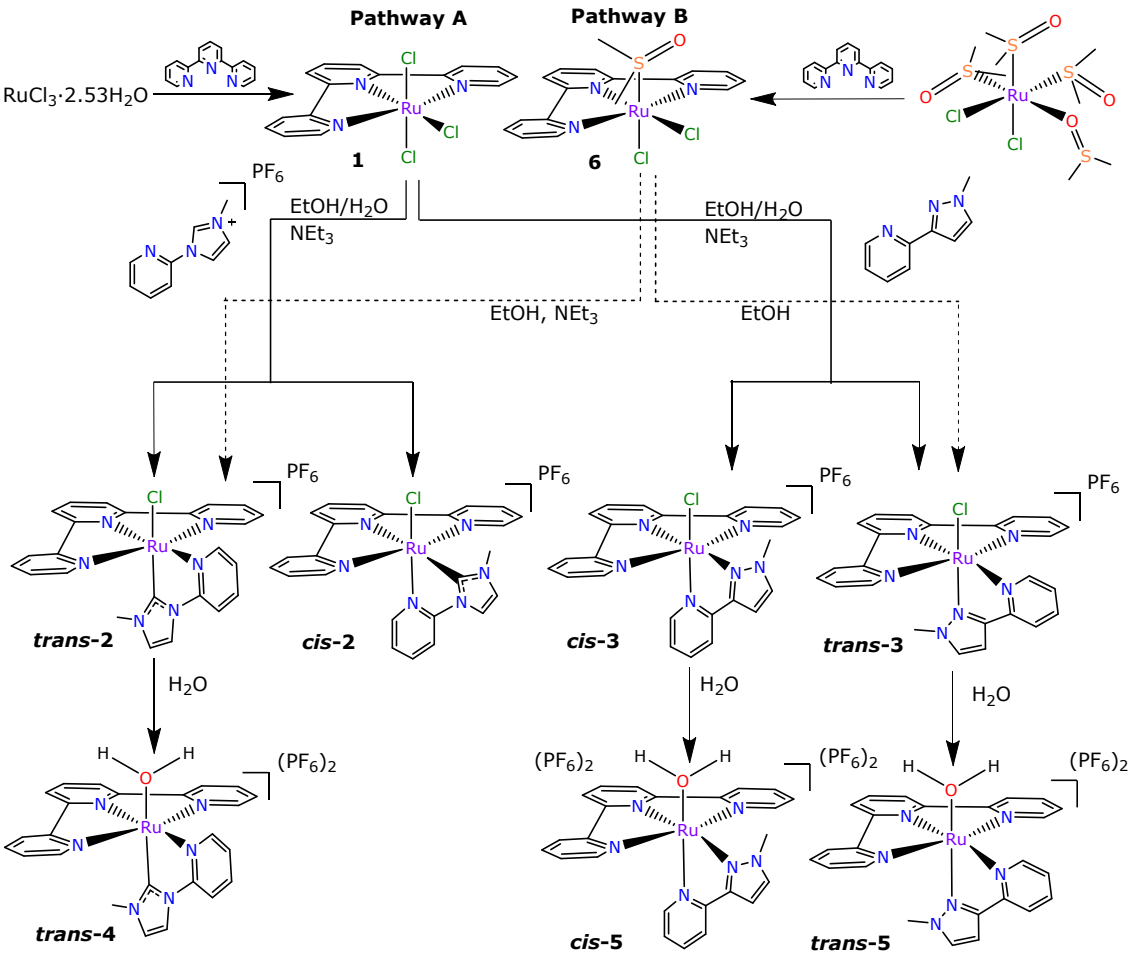

Figure 6. Synthetic scheme for the preparation of complexes. Pathway B for the synthesis of the chlorocomplexes 2 and 3 is indicated by dashed-line arrows.

In pathway A, the chlorocomplexes **2** and **3** are synthesized starting from the precursor **1** and NEt_3 to reduce Ru(III) to Ru(II) in EtOH/H_2O. In the case of complexes with the Cb-Me ligand, deprotonation of the imidazole C atom is necessary for coordination leading to the procedures described in the literature.[32 33]

For Cb-Me ligand, a 80:20 *trans*:*cis* mixture of chlorocomplex **2** is obtained through pathway A whereas it is around 1:1 for pypz-Me ligand of chlorocomplex **3**

Pathway B starts from Ru(II) complex **6**. This complex is obtained as a mixture of *cis* and *trans* isomers[31] (in this case the nomenclature refers to the relative position of the two Cl ligands) with a different ratio depending on the reaction time. If the raction takes place during 4 hours, it is mostly obtained the kinetically favoured isomer with a ratio 1:0.55 (*trans*/cis); if the raction takes place during 14 hours, it is mostly obtained the thermodynamically favoured isomer with a ratio 1:0.35. The isomeric mixture is used for synthesis. NEt_3 is added in the case of complex **2** to help deprotonation of Cb-Me. Yields are better through pathway B than A probably for the absence of $[Ru(trpy)_2]^+$ byproduct. We have the hypothesis that the reason why there is not $[Ru(trpy)_2]^{2+}$ formation could be for kinetically effects: DMSO ligand is more labile than cloro ligand leading to the formation of chlorocomplex instead of the $[Ru(trpy)_2]^{2+}$ formation.

Pathway B leads to isomerically pure *trans*-**2** and *trans*-**3** chlorocomplexes. A possible reason is that, in the starting complex **6**, DMSO decoordination (TS1) is presumably easier than Cl decoordination (TS2) (**Figure 7**). After dmso decoordination, the bonding of the bidentate ligand will probably take place through attack of the five-membered ring of Cb-Me or pypz-Me ligand (which have higher basic character) at the vacant position, then resulting in a *trans* chlorocomplex.

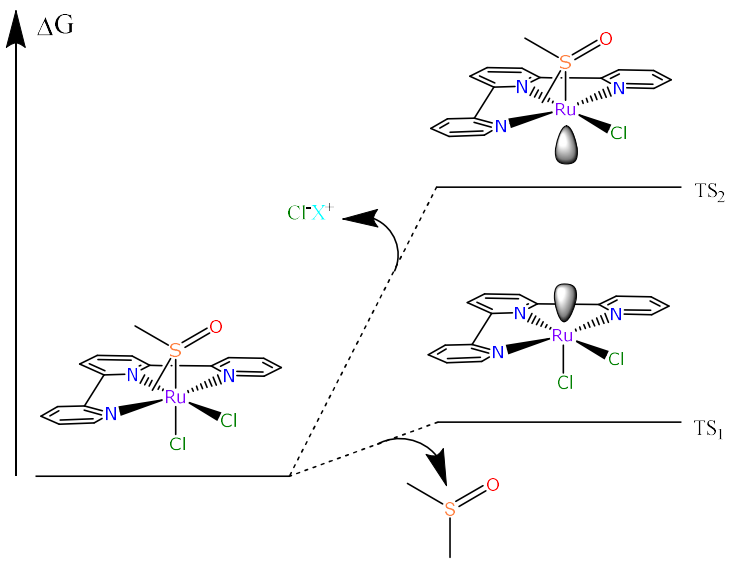

Figure 7 Proposed mechanism of Pathway B

Aqua complexes **4** and **5** are easily obtained by refluxing the corresponding chlorocomplex (**2** and **3** respectively) in water under N_2 atmosphere. The synthesis of ruthenium aquacomplexes is traditionally carried out using Ag^+ salts to help Cl ligand substitution by solvent through of AgCl, and in the synthesis of **4** and **5** previously reported[32 33]used $AgPF_6$ as reagent, but the

synthesis described in this work leads to the aquacomplexes through a cleaner procedure, with good yields.

^{1}H-NMR characterization

For the NMR assignment, the numbering scheme shown in Figure 8 has been used.

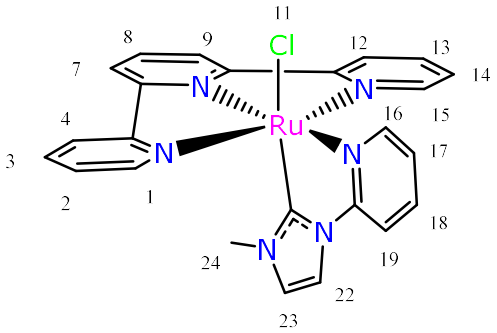

Figure 8. General numbering scheme for the C and H atoms of chloro and aqua complexes 2-5 as well as for the trpy ligand in the precursor complex 6.

As mentioned above, the precursor complex **6** is obtained as a mixture of *cis*-Cl and *trans*-Cl isomers in a different ratio depending on the reaction time. After 14 hours it mostly corresponds to the thermodynamically favoured conformation that is the *cis* isomer with a ratio of 1:0.35 (*cis/trans*) ; after 4 hours it mainly corresponds to the kinetically favoured conformation that is the *trans* isomer with a ratio 1:0.55 (*trans*/cis).

The complexes ***trans*-2**, ***cis*-2**, ***trans*-3** and ***cis*-3** were also characterized by ^{1}H-NMR coinciding to the spectrum described in the literature.[32 33] As it was mentioned above, the isomers ***trans*-3** and ***cis*-3** couldn't be separated but we could assign our chemical shifts of our spectrum (**Figure 6**) comparing to the NMR's of the isolated isomers with a ratio 1:0.66 (*trans*/cis).

The ^{1}H-NMR spectra of *trans*-chlorocomplexes are particular because there is an unshielded chemical shift. For example, ^{1}H-NMR of the mixture of ***trans*-3** and ***cis*-3** (Figure 6) has a chemical shift at 10.2ppm corresponding to the hydrogen in alpha position of pyridine ring. It is due to the proximity of the hydrogen and the chloro ligand. For the same reason, the methyl groups have different chemical shifts depending on the isomer: 3.05 ppm for *trans* isomer and 4.72 ppm for *cis*.

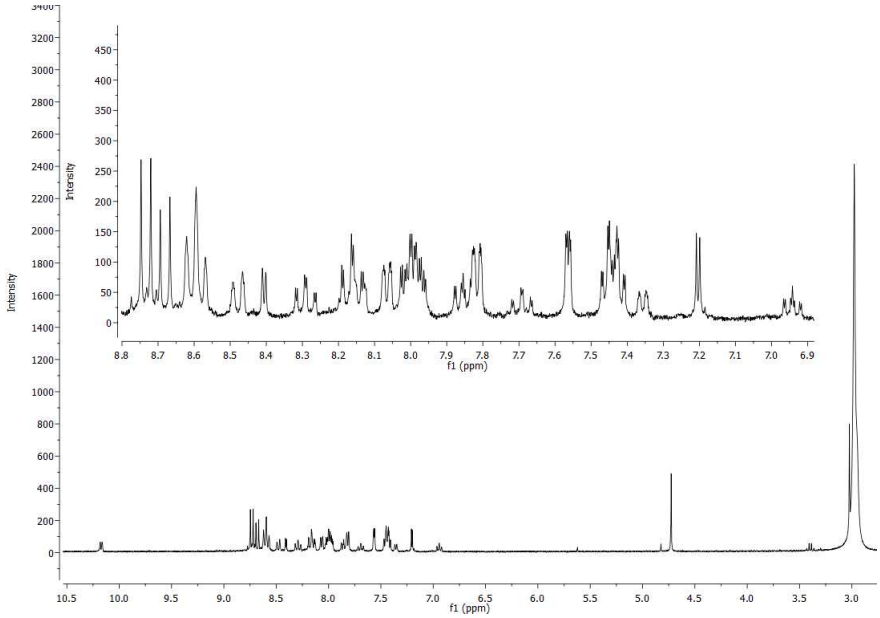

Figure 9 ^{1}H-NMR of the mixture of complexes 3-*trans* and 3-cis in acetone-d_6

The aqua complexes ***trans*-5** and ***trans*-5** also were characterized by ^{1}H-NMR. As well as for the chlorocomplexes, the spectrums coincides to the ones described in the literature.[32 33] *Trans*-aquocomplexes also have the characteristic unshielded chemical shift, at 9.5 ppm, but at minor ppm than the chlorocomplexes . This is due to the higher unshielding capacity of the chloro ligand compared to the aqua ligand. For the same reason, the methyl groups also appears at lower ppm (Figure 10).

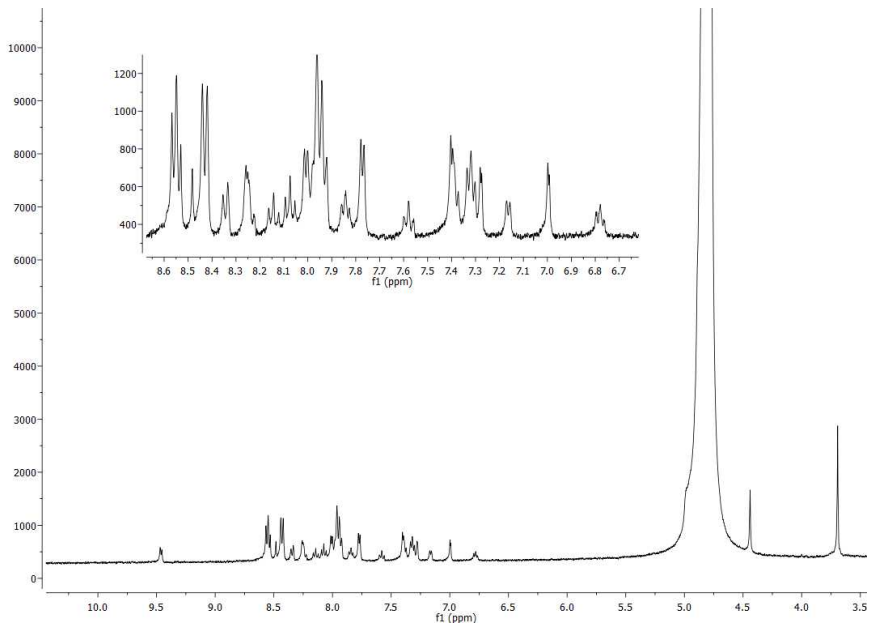

Figure 10 ^{1}H-NMR spectrum of 5-cis and 5-*trans* in D_2O

4.2. UV-vis spectroscopy.

The UV-VIS spectra of all the chlorocomplexes and aquocomplexes have been registered in dichloromethane and are according with the ones described in the literature.[32 33] Figure 11 displays the spectra obtained for 10^{-4} M solutions of the *trans*-chloro and aqua complexes containing the pypz-Me ligand, ***trans*-3** and ***trans*-5**. There are two types of *trans*itions:the π→π* *trans*itions, which appear in the range from 225nm to 325nm and are related with intramolecular *trans*itions of the polypyridyl ligands, and the MLCT, which appear in the range from 325nm to 525nm.

As it is clear in Figure 8, the *trans*itions π→π* are similar for either chlorocomplex and aquocomplex because is an intramolecular *trans*ition of the ligand and the structure of polypyridyl ligands is essentially maintained. However, the MLCT *trans*itions are more energetic in aquocomplex than chlorocomplex because the anionic chloro ligand has π-donor character, and, consequently, there is a desestabilization of the d(π) orbitals of Ru.

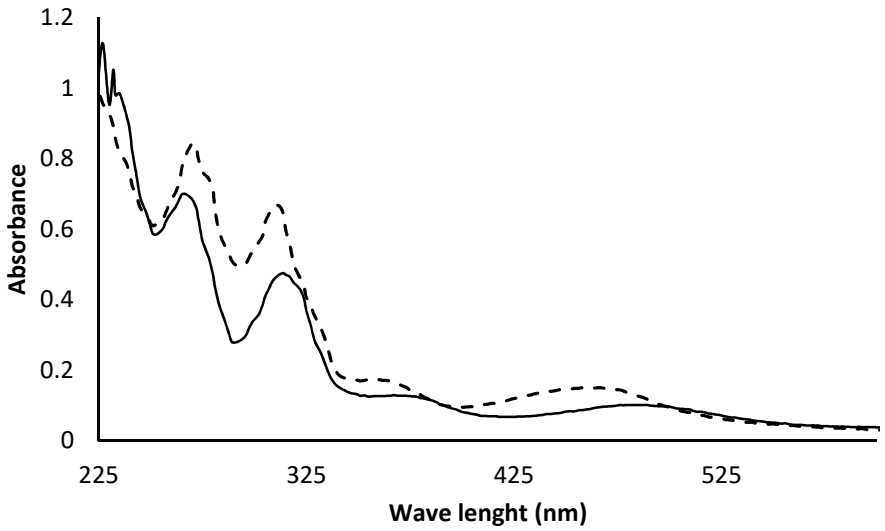

Figure 11 UV-Vis spectrums of *trans*-3 (solid line) CH_2Cl_2 and *trans*-5 (dashed line) in phosphate buffer.

The UV-vis spectra of the corresponding *cis* isomers as well as those of the complexes containing the carbene Cb-Me ligand display similar features.

4.3. Electrochemical characterization.

The redox properties of complexes **2**-**6** have been determined by CV and DPV experiments. In the case of complex **6**, the cyclic voltammetry of a mixture of *cis* and *trans* isomers is shown in Figure 12. Two electrochemically reversible waves can be observed, with $E_{1/2}$ values of 0.67 and 0.86 V vs SCE, corresponding to the Ru(III/II) redox pair of the *trans* and *cis* isomers respectively.

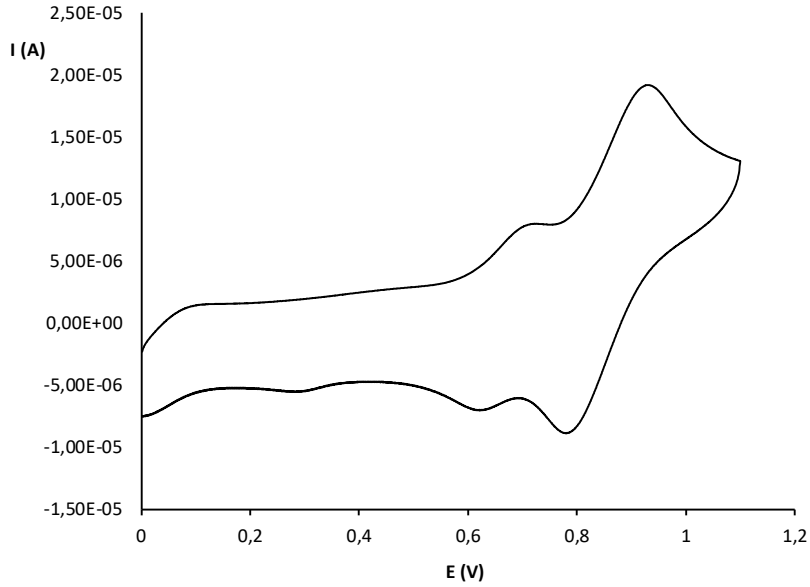

Figure 12. Cyclic voltammetry of a mixture of *cis* and *trans*-6 in dichloromethane with 0.1 M TBAH.

An additional cathodic peak can be observed at $E_{P,A}$ = 0.28 V, indicative of a Ru-S_{DMSO} → Ru-O_{DMSO} linkage isomerization process. This type of processes take place upon Ru^{II}→Ru^{III} oxidation, due to the increased hard Lewis acid character of the oxidized Ru(III) which displays more affinity for O-bonded DMSO, a harder Lewis base. This linkage isomerization is reversed after back-reduction to Ru(II). The processes involved and the corresponding kinetic and equilibrium constants are shown in Figure 13:

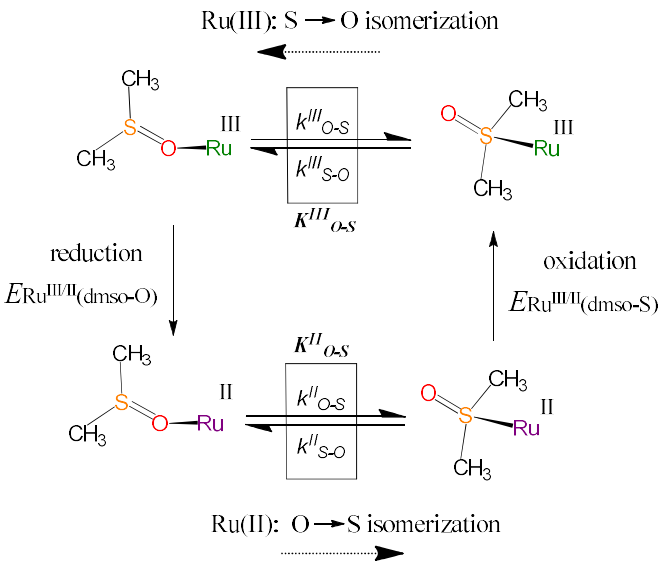

Figure 13. Kinetic and equilibrium constants involved in DMSO linkage isomerization of ruthenium complexes.

The equilibrium and rate constants can be determined by cyclic voltammetries at different scan rates, as described in the experimental

section. CVs have been performed for a mixture of *cis*- and *trans*-**6** complexes in dichloromethane at scan rates from 0,02 to 0,8 V/s, with starting potentials at the lower or upper points of the potential range. The cyclic voltammetries obtained are displayed in Figure 14:

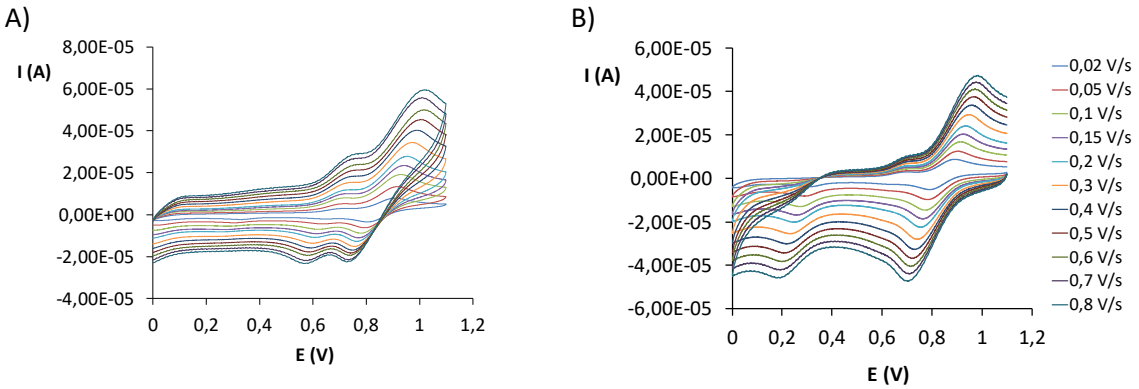

Figure 14. Cyclic voltammetries performed for an isomeric mixture of *cis* and *trans*-6 in dichloromethane containing 0.1M TBAH at different scan rates between 0,02 and 0,8 V/s. A), anodic (direct) scans; B), cathodic (reverse) scans.

As can be observed in Figure 14B, the cyclic voltametries carried out starting by cathodic scans display an increased intensity of the cathodic peak at 0.28 V, in parallel with a decrease in the intensity of the reduction corresponding to the *trans* isomer, for which the cathodic Ru(III)→Ru(II) peak disappears at scan rates above 0.1 V/s. To calculate the corresponding rate and equilibrium constants, the cathodic and anodic intensity values were analyzed through linear regression of equations 1-4 (see experimental section). The values obtained are gathered in Table 2 (entry 1), together with other Ru-dmso complexes described in the literature.

Table 2. Thermodynamic and kinetic parameters for the linkage isomerization of complex *trans*-6, together with related Ru-dmso complexes.[a]

Entry	Compound	K^{II}_{O-S}	k^{II}_{O-S} (s^{-1})	k^{II}_{S-O} (s^{-1})	K^{III}_{O-S}	k^{III}_{O-S} (s^{-1})	k^{III}_{S-O} (s^{-1})
1	*trans*-[$RuCl_2$(trpy)(dmso)], ***trans*-6**	$4.87\cdot10^{4}$	$4.0\cdot10^{-4}$	$8,2\cdot10^{-9}$	0.018	$3.5\cdot10^{-2}$	1.97
2	*cis,cis*-[$RuCl_2$(pypz-H)(dmso-S)$_2$] (ref 10a)	$1.34\cdot10^{12}$	$1.1\cdot10^{-1}$	$8.2\cdot10^{-14}$	1.39	$1.8\cdot10^{-1}$	$1.26\cdot10^{-1}$
3	*cis,cis*-[$RuCl_2$(H3p)(dmso-S)$_2$] (ref 10b)	$5.2\cdot10^{11}$	$4.9\cdot10^{-1}$	$9.3\cdot10^{-14}$	1.70	$2.8\cdot10^{-1}$	$1.7\cdot10^{-1}$
4	*trans,cis*-[$RuCl_2$(H3p)(dmso-S)$_2$] (ref 10b)	$5.3\cdot10^{8}$	$8.7\cdot10^{-2}$	$1.6\cdot10^{-10}$	0.27	$5.7\cdot10^{-2}$	$2.2\cdot10^{-1}$
5	*trans,cis*-[$RuCl_2$(bpp)(dmso-S)$_2$]$^-$ (ref 10c)	$6.5\cdot10^{9}$	$1.3\cdot10^{-1}$	$2.1\cdot10^{-11}$	0.26	$1.7\cdot10^{-2}$	$6.5\cdot10^{-2}$
6	*out*-[Ru(L^2)(trpy)(dmso-S)]$^+$ (ref 10d)	$5.5\cdot10^{8}$	$2.5\cdot10^{-1}$	$4.6\cdot10^{-10}$	0.13	$7.7\cdot10^{-2}$	$6.0\cdot10^{-1}$
7	*cis,fac*-[$RuCl_2$(CH_3-pz-H)(dmso-S)$_3$] (ref 10a)	$1.53\cdot10^{12}$	$7.2\cdot10^{-2}$	$4.7\cdot10^{-14}$	0.036	$1.9\cdot10^{-2}$	$5.3\cdot10^{-1}$

[a]*pypz-H* is 3-(2-pyridyl)-1H-pyrazole, *H3p* is 5-phenyl-3-(2-pyridyl)-1H-pyrazole, L^2 is 5-phenyl-3-(pyridin-2-yl)pyrazolate and *bpp* is 3,5-(2-pyridyl)pyrazolate.

As can be observed in Table 2, the values of K^{II}_{O-S} obtained for all complexes are very high indicating that, in Ru(II) redox state, the dmso

ligand displays a high preference to be bound to the metal through the S atom (see Table 2). However, the value displayed by complex ***trans*-6** is markedly minor to that shown by the rest of compounds. This indicates a relatively lower thermodynamic stability of ***trans*-6** when compared to other Ru-S_{dmso} complexes, which could be explained by both steric and electronic factors. First, from a structural perspective, the coordination through the S atom places the two dmso methyl groups close to the metal in the plane defined by the rigid trpy ligand, whereas the O-coordination would move them away from the Ru center then diminishing the steric encumbrance. On the other hand, regarding electronic factors, the S-bound dmso, which displays a high π-acceptor character, is situated in *trans* to a pyridyl ring that is also a π-acceptor. This is an energetically unfavorable disposition, with the two ligands bonding to the same **d** orbital (in the rest of complexes of Table 2 the dmso ligands is situated in *trans* to either Cl or pyrazolyl ligands). Linkage isomerization seems to be favored in this case thanks to the lower π-acceptor character of the O-bound dmso, which is originated from the absence of empty **d** orbitals at the oxygen atom in contrast to what happens in S-bound DMSO.

The factors described above would also explain the $K^{III}_{O\text{-}S}$ value of 0.018, the lowest among all the complexes in Table 2, evidencing that the Ru-O_{DMSO} form dominates over the Ru-S_{DMSO} in the Ru(III) oxidation state. Steric factors are probably even more important for Ru(III) than for Ru(II) due to the decrease of the metal ionic radius upon oxidation.

Regarding the kinetic constants, the values displayed by ***trans*-6** in Ru(II) oxidation state indicate that the Ru-O→Ru-S isomerization process ($k^{II}_{O\text{-}S}$) is particularly slow when compared to the rest of complexes, and the Ru-S→Ru-O conversion shows the highest $k^{II}_{S\text{-}O}$ value (although it is only around 10^{-9} s^{-1}). For Ru(III), the $k^{III}_{O\text{-}S}$ value is similar to those of other Ru-DMSO compounds, but the $k^{III}_{S\text{-}O}$ value of 1.97 s^{-1} is particularly high, again indicating that the Ru-S→Ru-O isomerization is highly favored in complex ***trans*-6**. This is in accordance with the cathodic scan CVs registered for the complex (Figure 14B), where the cathodic peak corresponding to the Ru^{III}-S→Ru^{II}-S reduction process in the *trans* isomer is only hardly observed.

Finally, in the ***cis*-6** isomer the π-acceptor S-DMSO ligand is in *trans* to a π-donor Cl ligand and is also out of the *trpy* ligand plane. Both factors seem to increase the thermodynamic and kinetic stability of this isomer, which does not display any linkage isomerization process.

Regarding the chloro and aqua complexes **2-5**, the $E_{1/2}$(III/II) of cyclic voltametries of all complexes are according to potentials described in the literature. [32 33]

The CV obtained in dichloromethane for the chloro complexes **2** and **3** are shown in Figure 15. The ***trans*-2** complex has the higher $E_{1/2}$ and the mixture of ***cis*-3** and *trans*-3 is the lower one. We have the hypothesis that Ru(III/II) potential differences between *trans*-2, *cis*-2 is occasioned by Ru-Cl bond length, which are 2.470Å and 2.386Å.[32] When the chloro ligand is further, it takes off more electronic density increasing the Ru(III/II) potential.

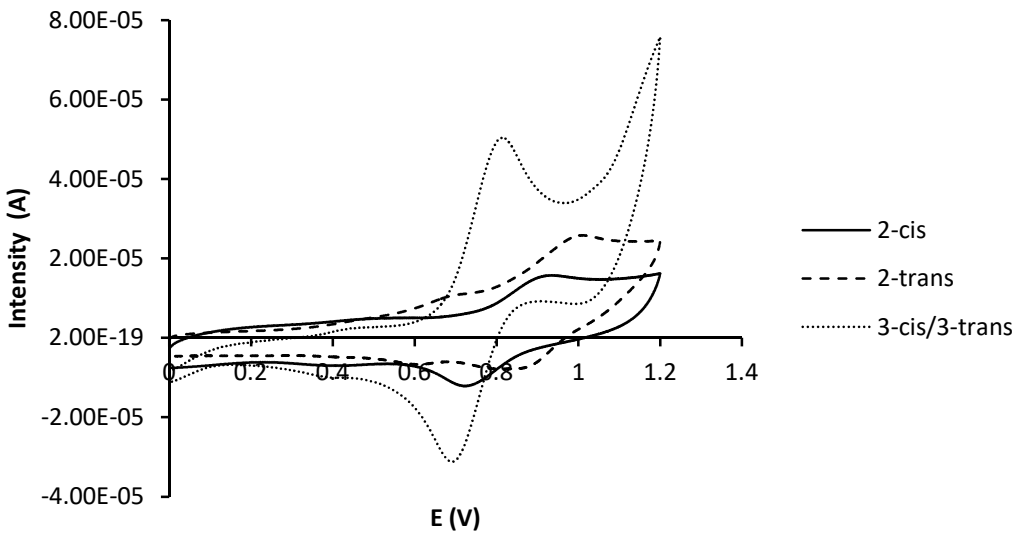

Figure 15. CV of *cis*-2, *trans*-2 and the mixture of *cis* and *trans*-3 in CH_2Cl_2+0.1M TBAH.

The electrochemical characterization of *trans*-4 and *cis*-5/*trans*-5 is performed in phosphate buffer of pH = 7.02. The DPV performed on a mixture of *cis*-5/*trans*-5 shows three different waves (Figure 16): for *trans*-5, the Ru(III/II) and the Ru(IV/III) redox processes take place at 0.38 V and 0.60 V respectively. For *cis*-5, a single wave at 0.50V is observed, which corresponds to a bielectronic Ru (IV/II) redox. The potential values were in accordance with the literature results.[32 33]

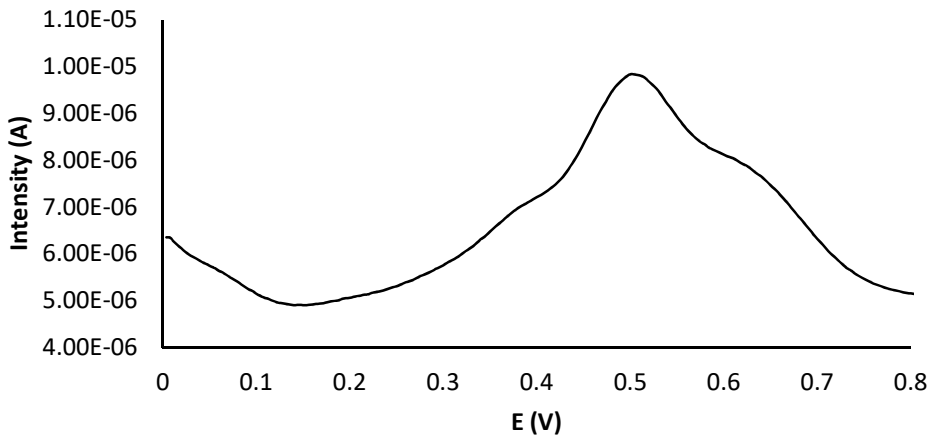

Figure 16. DPV of cis-5/*trans*-5 mixture in phosphate buffer pH=7.02.

On the other hand, the CV of *trans*-4 shows an unique bielectronic wave corresponding to the Ru(IV/II) coupling at 0.60V (see Figure 17). The potentials of aquacomplexes are lower than chlorocomplexes because the oxidation of ruthenium goes in parallel with the desprotonation of aqua ligand and it favours the process.

As mentioned in the introduction, aquacomplexes undergo PCET processes with pH-dependent potential values. Figure 17 shows the CVs of *trans*-4 at different pH values and, as can be observed, the Ru(IV/II) redox potential is higher at pH = 2 than in neutral conditions, in consistency with Nernst equation.

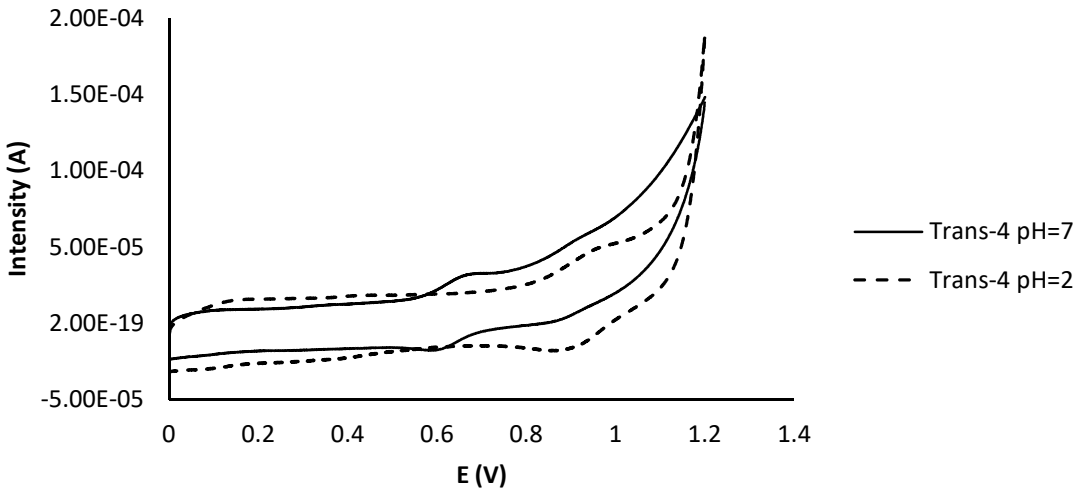

Figure 17. CV of *trans*-4 at different pH

4.4. Photocatalytic oxidation alcohol reactions

The photocatalytic reactions were carried out with primary and secondary alcohols with different types of substituent with $Na_2S_2O_8$ as sacrificial oxidant and $[Ru(bpy)_3]Cl_2$ as photosensitizer agent during 15 hours using *trans*-4 and a mixture of *cis*-5/*trans*- 5 as catalytic agent. Also, we have done 2 blank tests: one without photosensitizer and, the other, without catalyst. The results are presented in **Table 3:**

Table 3. Photocatalytic results of *trans*-4 and *cis*-5/*trans*-5.[a]

Entry	Substrate	trans-4			cis-5/trans-5		
		Conversion (%)	Selectivity (%)		Conversion (%)	Selectivity (%)	
			Aldehyde/ketone	Carboxylic acid		Aldehyde/ketone	Carboxylic acid
1	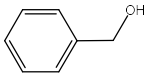	>99	5	34	>99	<2	96
2	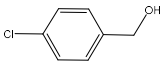	61	11	88	>99	9	91
3	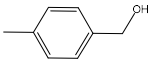	>99	43	45	>99	79	8
4	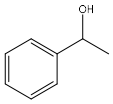	13	34	-	>99	<5	-
5	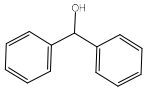	26	46	-	92	60	-

[a]1:10:100:200(catalyst:photosensitizer:substrate:sacrificial oxidant)

The conversions of all substrates were moderated-high for both cathalysts. However, the selectivities were low-moderated for aldehyde or ketone.

The catalyst *trans*-4 has good conversions for primary alcohols whereas the conversions for secondary alcohols are low. Nevertheless, the selectivites for the corresponding aldehyde or ketone are, in general, higher in secondary alcohols than in primary alcohols. The most primary alcohols convert to carboxylic acid.

The mixture of isomers *cis*-5/*trans*-5 has good conversions for primary and secondary alcohols but selectivity does not follow a clear tendency. It have to be note that the substrate 4 has low conversions. We could assign in ^{1}H-NMR spectrums the presence of one specie which has lost a methyl group.

The activity difference with both catalysts could be due to electronic factors. According to previous studies,[35] [36] a possible mechanism of alcohols oxidation of Ru^{IV}=O goes throw a Ru^{IV} heptacoordinated *trans*ition state which is shown in the Figure 18 species of involving a water molecule.

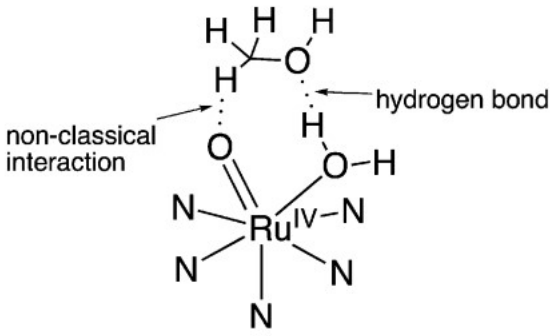

Figure 18 Transition state of RuIV=O in alcohol oxidation process.

Water molecule forms an hydrogen bond by the oxygen atom of the alcohol as well as the oxo group of the catalyst establishes a *non-classical interaction* with the alpha proton of the alcohol.

In one hand, the *trans*-4 has the σ-donor carbene ligand in *trans* to the oxo group, so, the Lewis acidity of ruthenium is reduced. Therefore, the coordination of the water molecule and the interaction between the oxo group and alpha proton of the alcohol is less favourable and the reactivity decreases. In the other hand, the mixture of isomers of complex 5, the ligand in *trans* could be a pyrazole (*trans*) or pyridine, which are less σ-donor , increasing the reactivity. It is also coherent with the values of pK_a of Ru^{II} aquacomplexes that in complex 4 are bigger, approximately one unit, than the mixture of isomers 5. [32] [33]

5. Conclusions

Two families of ruthenium chloro and aqua complexes, containing the tridentate trpy and the bidentate Cb-Me or pypz-Me ligands, have been synthesized through two different synthetic pathways. The complexes and the corresponding intermediate species have been fully characterized through spectroscopic and electrochemical techniques.

The synthetic pathway B, involving the synthesis of the intermediate complex [$RuCl_2$(trpy)(DMSO)], 6, leads to higher overall yields for the corresponding chlorocomplex, either when using Cb-Me or pypz-Me as bidentate ligand and, in both cases, the compound is obtained as pure *trans* isomer.

Complex 6 is obtained as a mixture of *trans*- and *cis*-Cl isomers in different ratio depending on the reaction time. The *trans* isomer is obtained in a higher amount for shorter reaction times, indicating that it is the kinetically favoured isomer.

The mono-dmso *trans* isomer of complex 6 undergoes a Ru-S_{DMSO}→Ru-O_{DMSO} linkage isomerisation process upon Ru(II)→Ru(III) electrochemical oxidation. The corresponding rate and equilibrium constants have been calculated, evidencing a kinetic $k^{III}_{O\text{-}S}$ value considerably higher to that displayed by bis-dmso compounds.

Aquacomplexes were obtained just refluxing the corresponding chlorocomplex in water under N_2 atmosphere, avoiding the use of silver salts which is carried out in traditional synthesis of related compounds.

The aquacomplexes 4 and 5 have been tested in the photocatalytic oxidation of primary and secondary alcohols to aldehydes or ketones respectively, displaying moderate to high conversion values with low to moderate selectivities. Carboxylic acids are obtained in the case of primary alcohols as byproducts.

The bidentate ligand (Cb-Me or pypz-Me) and the *cis* or *trans* geometry of the complexes influences the catalytic activity. The catalyst *trans*-4*,* having the most electron-donor carbene ligand in *trans* to the oxo group, displays the lower performance, whereas the isomeric mixture of complex 5 leads to excellent conversion values

6. Ethics and sustainability

In this work, we have founded a new synthetic route which has better yields than others described in the literature. So, this new route produces less residues. We also have test photocathalytic oxidations in water which are mild conditions with the aim to obtain sustainable pathways.

During the experimental part of this work, we have been using all the security elements needed and we have treated well all the residues.

In this work, all the information was searched in trustworthy sources and well indexed. So, there is not plagiarism.

7. Bibliography

[1] Whittall, I. R.; McDonagh, A. M.; Humphrey, M. G.; Samoc, M. *Adv. Organomet. Chem.* **1999**, *43*, 349.
[2] Larionova, J.; Mombelli, B.; Sanchiz, J.; Khan, O. *Inorg. Chem.* **1998**, *37*, 679.
[3] Perason, A. J.; Hwang, J. J. *Tetrahedron Lett.* **2001**, *42*, 3533.
[4] Espinet, P.; Esteruelas, M. A.; Oro, L. A.; Serrano, J. L.; Sola, E. *Coord. Chem. Rev.* **1992**, *117*, 215.
[5] Durham, B.; Caspar, J. V.; Nagle, J. K.; Meyer, T. J. *J. Am. Chem. Soc.* **1982**, *104*, 4803.
[6] Takeuchi, K. J.; Thompson, M.S.; Pipes, D.W.;Meyer, T.J. *Inorg. Chem.* **1984**, 23, 1845.
[7] Sens, C.; Romero, I.; Rodríguez, M.; Llobet, A.; Parella, T.; Benet-Buchholz, J. *J. Am. Chem. Soc.* **2004**, 126, 7798.
[8] Cao, R.; Wenzhen, L.; Du, P. *Energy Environ. Sci*., **2012**, 5, 8134
[9] Pearson, R. G. *J. Am. Chem. Soc.* **1963**, *85*, 3533.
[10] a) Ferrer, I.; Fontrodona, X.; Rodríguez, M.; Romero, I. *Dalton Trans.* **2016**, 45, 3163. b) Roeser, S.; Maji, S.; Benet-Buchholz, J.; Pons, J.; Llobet, A. *Eur. J. Inorg. Chem.* **2013**, *2*, 232. c) Sens, C.; Rodríguez, M.; Romero, I.; Llobet, A.; Parella, T.; Sullivan, B. P.; Benet-Buchholz, J. *Inorg. Chem.* **2003**, *42*, 2040-2048. d) Benet-Buchholz, J.; Comba, P.; Llobet, A.; Roeser, S.; Vadivelu, P.; Wiesner, S. *Dalton Trans.* **2010**, 39, 3315.
[11] a) Sens, C.; Rodríguez, M.; Romero, I.; Llobet, A.; Parella, T.; Sullivan, B. P.; Benet-Buchholz, J. *Inorg. Chem*. **2003**, *42*, 2040. b) Shan, N.; Adams, H.; Thomas, J. A. *Inorg. Chim. Acta* **2006**, *359*, 759. c) Okumura, T.; Morishima, Y.; Shiozaki, H.; Yagyu, T.; Funahashi, Y.; Ozawa, T.; Jitsukawa, K.; Masuda, H. *Bull. Chem. Soc. Jpn.* **2007**, *80*, 507.
[12] Khan, M. M. T.; Mohiuddin, R.; Vancheesan, S.; Swamy, B. *Ind. J. Chem. Section A: Inorg., Phys., Theor.& Anal.* **1981**, *20A*, 564.
[13] Ferrer, I.; Rich, J.; Fontrodona, X.; Rodríguez, M.; Romero, I. *Dalton Trans.* **2013**, 42, 13461
[14] Wang, L.; Duan, L.; Stewart, B.; Pu, M.; Liu, J.; Privalov, T.; Sun, L. *J. Am. Chem. Soc.* **2012**, *134*, 18868.
[15] Khenkin, A. M.; Shimon, L. J. W.; Neumann, R. *Inorg. Chem.* **2003**, *42*, 3331.
[16] Bratsos I.; Bergamo, A.; Sava, G.; Gianferrara, T.; Zangranado, E.; Alessio, E. *Inorg. Biochem.* **2008**, 102, 606.
[17] Bourissou, D.; Guerret, O.; Gabbaï, F.P.; Bertrand, G. *Chem. Rev.* **2000**, 100, 39.
[18] Zhao, S.; Wu, J.; Chen, W. *J. Org. Chem.* **2017**, 249.
[19] Drozdzak, R.; Allaert, B.; Ledoux, N.; Dragutan, I.; Dragutan, V.; Verpoort, F. *Coord. Chem. Rev.* **2005**, 249, 3005.
[20] Liu, H.J.; Gil-Sepulcre, M.; Francàs, L.; Nolis, P.; Parella, T.; Benet-Buchholz, J.; Fontrodona, X.; García-Antón, J.; Romero, N.; Llobet, A.; Escriche, L.; Bofill, R.; Sala, X. *Dalton Trans.* **2017**, 46, 2829.
[21] Lheman, S.E.; Wagener, K.B.; *Organometallics* **2005**, 24, 1477
[22] Twilton, J.; Le C.; Zhang, P.; Shaw, M.H.; Evans, R.W.; MacMillan, D.W.C. *Nature Rev*. **2017**, 1, 1.
[23] Zhang, X.; Ke, X.; Yao, J. *J. Mater. Chem. A.* **2018**, 6, 1941.

[24] Jurss, J.W.; Khanayzer, R. S.; Panetier, J. A.; El Roz, K. A.; Nichols, E. M.; Head-Gordon, M.; Long, J. R.; Castellano, F. N.; Chang, C. J.; *Chem. Sci.* **2015**, 6, 4954.
[25] Ferreira, K.N.; Iverson, T.M.; Maghlaoui, K.; Barber, J.; Iwata, S.; *Science*, **2004**, 303, 1831.
[26] Li, T.; Li, F.; Zhao, W.; Tian, Y.; Chen,Y.; Cai, R., Fu, W. *Inorg. Chem.* **2005**, 54, 183.
[27] Grüdemann, S.; Kovacevic, A.; Albercht, M.; Faller, J. W.; Crabtree, R. H. *J. Am. Chem. Soc.* **2002**, 124, 10473
[28] Rieb, J; Raba, A.; Haslinger, S.; Kaspar, M.; Pöthig, A.; Cokoja, M.; Basset, J. M.; Kühn, F.; *Inorg. Chem.* **2014**, 53, 9598
[29] Thiel, W.R.; Angstl, M.; Priermeier, T.; *Chem. Ber,* **1994**, 127, 2373.
[30] Sullivan, B.P.; Calvert, J.M.; Meyer, T.J.; *Inorg. Chem.* **1980**, 19, 1404.
[31] Ziessel,R.; Grosshenny, V.; Hissler, M.; Stroh, C. *Inorg. Chem.* **2004**, 43, 4262.
[32] a) Dakkach, M.; Atlamsani, A.; Parella, T.; Fontrodona, X.; Romero, I.; Rodríguez, M; *Inorg. Chem.* **2013**, 52, 5077. b) Dakkach, M.; Fontrodona, X.; Parella, T.; Atlamasani, A.; Romero, I.; Rodríguez, M.; *Adv. Synth. Catal.* **2011**, 353, 231.
[33] Dakkach, M.; Lopez, M.I.; Romero, I.; Rodríguez, M.; Atlamsani, A.; Parella, T.; Fontrodona, X.; Llobet, A. *Inorg.Chem.* **2010**, 49, 7072.
[34] Nicholson, R. S.; Shain, I. *Anal. Chem.* **1964**, *36*, 706-723.
[35] Ishizuka, T.; Kotani, H.; Kojima, T. *Dalton Trans.* **2016**, 45, 16727.
[36] Ohzu, S.; Ishizuka, T.; Hirai, Y.; Jiang, H.; Sakaguchi, M.; Ogura, T.; Fukuzumi, S.; Kojima, T. *Chem. Sci.* **2012**, 3, 3421.